

The effect of various sulfides on carbon deposition on nickel–iron particles

Cher D. Tan*, R. Terry K. Baker

Department of Chemistry, Northeastern University, Boston, MA 02115, USA

Received 23 September 1999; accepted 24 January 2000

Abstract

The amount and degree of graphitic character of the carbon deposits formed on Fe–Ni (1:4) particles when heated in an ethane/steam environment at temperature ranging from 765 to 925°C was found to be dependent upon the concentration as well as the chemical nature of the sulfide species present in the reactant stream. Distinct advantages with regard to inhibition of carbon deposition were found when either dimethyl sulfide (DMS) or dimethyl disulfide (DMDS) were used as additives to the reactant mixture compared to the behavior observed with H₂S. The introduction of 25 ppm of the organic sulfides produced a significant decrease in the formation of catalytically generated carbon and a corresponding increase in the yield of the desired product ethylene. Under the same conditions H₂S was found to promote the growth of catalytic carbon at the expense of ethylene production. Electron microscopy examinations showed that the addition of sulfur species to the reactant feed created a major change in the structural characteristics of the solid carbon deposit as the temperature was progressively raised from 765 to 925°C. At temperatures in excess of 865°C there was a transformation from filamentous to graphitic shell-like structures. The ramifications of this phenomenon on the operation of commercial reactor systems is discussed. © 2000 Published by Elsevier Science B.V.

Keywords: Sulfides; Carbon; Nickel–iron particles

1. Introduction

Carbon deposition on catalysts, reactor tubes and heat exchanger surfaces adversely affects the performance of a large number of industrial processes, particularly those involving the conversion of hydrocarbons. Several review articles have highlighted the complex structure of carbon deposits [1–8], which can be divided into three main classes: amorphous or pyrolytic, filamentous and graphite shell-like structures. These different types would not be distinguished during a routine analysis of a carbonaceous deposit, but merely referred to collectively as “coke”. The potential for carbon formation exists in any system in which

hydrocarbons undergo thermal decomposition and it is well known that certain metals can increase the overall rate of this process by catalyzing the growth of filamentous and the graphitic types of deposit. The highest catalytic activity for carbon deposition is exhibited by iron, cobalt, nickel, and alloys containing these metals.

The available evidence suggests that the amorphous carbon component is formed via condensation and polymerization reactions and this material originates from thermal processes. It is conceivable that a significant amount of hydrogen is incorporated in the deposit, however, as the temperature is raised dehydrogenation reactions will tend to reduce the hydrogen content [9]. It is also believed that the acidic nature of a surface can have a profound effect on the

* Corresponding author.

amount of this type of carbon that accumulates [10]. On the other hand, there is a general consensus that the formation of the filamentous and graphitic forms of carbon require the participation of a catalytic entity that usually operates in a particulate form during the respective growth processes.

The mechanism commonly accepted to account for the observed characteristics of the steady-state growth of carbon filaments from the metal catalyzed decomposition of carbon-containing gases can be summarized according to the following steps [11,12]:

1. adsorption of reactant gas molecules at particular faces of the metal particle followed by decomposition to generate carbon species;
2. dissolution in and diffusion of carbon species through the metal particle;
3. precipitation of carbon from a different set of faces to form a fibrous structure.

It has been established that the latter set of faces control not only the degree of crystalline perfection of the deposited carbon filament, but also the conformational characteristics of the material [13–16]. A consequence of this phenomenon is that certain metal faces will remain free of deposited carbon and therefore, available for continued reaction with the hydrocarbon.

While the fundamentals of the formation of the graphite shell-like deposit have not received the same attention as the efforts devoted to the growth characteristics of filamentous carbon there is a possibility that many of the steps outlined above are also involved in the formation of this type of carbon. Nolan et al. [17] reported that graphite, in the form of a shell structure surrounding a metal particle core, was the exclusive type of deposit produced from the decomposition of carbon monoxide. They observed that the limiting thickness of the graphite shells was about 30 layers, and that this parameter was dependent on the lifetime of the metal catalyst particles. Based on these findings, they argued that the growth of graphite layers did not occur via a mechanism that involved precipitation of carbon from the surface of the metal. Rodriguez et al. [18] carried out a detailed examination of the nature of the solid carbon produced on iron–nickel particles during interaction with ethane at about 850°C, conditions at which the alkane readily forms ethylene, and demonstrated that precipitation of dissolved species was the key step in the formation of the graphitic shell-like deposits.

Previous work from this laboratory [19–21] has shown that either pre-treatment or continuous addition of 5–10 ppm H₂S to iron, nickel or cobalt particles undergoing reaction with ethylene had a significant impact on the catalytic activity of these metals, particularly with respect to the enhancement in yields of carbon filaments. It should be emphasized that while trace amounts of sulfur in the gas stream can promote carbon deposition on metal particles, it is well established that high levels of sulfur-containing additives effectively inhibit its accumulation [22–28]. In the current investigation, we have extended this experimental approach in an attempt to establish the effect of the chemical nature of the sulfur precursor molecule on the characteristics of the carbon deposit resulting from the iron–nickel catalyzed decomposition of ethane. Attention has been focused on a number of factors that could have an impact on this phenomenon including, the reaction temperature, the chemical nature of the sulfur precursor molecule, the concentration of the additive and the characteristics of the solid carbon deposit.

Motojima et al. [29,30] have examined the effects of a variety of sulfur compounds, including H₂S, *n*-butylmercaptane, dibenzylsulfide and thiophene, as additives to acetylene for the growth of carbon filaments from nickel powders at temperatures ranging from 550 to 750°C and 1 atm pressure. They reported that there were significant differences in the behavior of the sulfur compounds on this reaction and that thiophene was the most effective for the growth of coiled carbon filament structures. The optimum yield (about 50 wt.%) for the growth of these carbon structures was obtained at a thiophene flow rate of 0.35 sccm (1.17% in acetylene). It was claimed that the optimum flow rate of the additive was restricted to a very narrow range and that “excessive” amounts of this component might act as poisons for the nickel catalyst. It was significant that these workers found that the yield of carbon filaments produced by this method was 1.7 times greater than that obtained from using H₂S as the additive molecule.

Kato et al. [31] studied the catalytic effect of sulfurized metal and sulfur-containing substrates for growth of vapor grown carbon fiber production at temperatures around 1100°C and 1 atm pressure. They claimed that the catalyst, which had equivalent amounts of sulfur and metal was in the molten state under these conditions. Egashira et al. [32,33]

found that carbonaceous substrates containing 3% sulfur and sulfur pretreated ceramic materials such as alumina and silica exhibited high activity for carbon filament formation. When the sulfur-containing substrates were impregnated with a fine dispersion of iron there was a significant increase in the yield of the solid carbon product. They rationalized the promotional effect of sulfur according to the notion that the formation of HS radicals in the vapor phase resulted in the extraction of hydrogen from the edges of the growing carbon fiber to generate active centers that facilitated the deposition of further amounts of solid carbon. While this explanation may be somewhat questionable, the experimental observations are certainly relevant to the current investigation.

2. Experimental

2.1. Flow reactor studies

A flow unit was specially designed and constructed to allow for the introduction of a reactant mixture (ethane/steam/sulfides/helium) to a quartz tube (40-mm ID and 90-cm long) that was heated by a conventional Lindberg horizontal tube furnace. The gas flow to the reactor was accurately monitored and regulated by the use of MKS mass flow controllers. Powdered Fe–Ni (1:4) catalyst samples (100 mg) were dispersed along the bottom of a ceramic boat, which was placed at the center of the quartz reactor tube. After reduction in a 10% H₂–He (20:180 cm³/min) mixture at 600°C for 1.0 h, the reactor was purged with helium while the system was brought to the desired reaction temperature (765–925°C). The reactant mixture ethane/steam (4:1) (200 cm³/min) containing various amounts of sulfide species was introduced into the reactor. After a reaction period of 2.0 h, the system was once again purged with helium and then allowed to cool down to room temperature. There was provision for taking gas samples at various intervals during reaction for subsequent product analysis by a Varian 3400 Gas Chromatography unit that was equipped with a 30-m megabore (GS-Q) capillary column.

2.2. Characterization studies of solid carbon deposits

The characterization studies of the solid carbon deposits produced on the alloy powder were performed

using a combination of techniques including, high resolution transmission electron microscopy and temperature programmed oxidation. The detailed structural features of the carbonaceous deposits were determined from examinations performed in a JEOL 2000EX II electron microscope. The lattice resolution of this instrument is estimated to be 0.18 nm. The degree of crystalline order of individual forms of the deposit was ascertained from selected area electron diffraction analysis and lattice fringe measurements. Suitable specimens for transmission purposes were prepared by ultrasonic dispersion of the deposit in iso-butanol followed by application of a drop of the supernatant onto a holey carbon support film. With this type of specimen arrangement it was possible to find sections of the deposit which were extremely thin and protruded from the edge of the carbon support film.

The graphitic content of the various samples of carbonaceous deposits was evaluated from a comparison of the oxidation characteristics of such materials with that of two standard materials, high purity single crystal graphite and active carbon in a CO₂/Ar (1:1) mixture. These experiments were carried out using a Cahn 2000 microbalance in which the specimen was heated at a rate of 5°C/min. Under these conditions the onset of gasification of active carbon took place at 550°C, whereas the corresponding point for pure graphite was found to be 860°C. Prior to conducting the oxidation experiments all metallic inclusions were removed from the deposits by repeated washing in 1 M HCl over a period of 7 days. The efficiency of this process was checked by XRD and TEM examinations of the treated deposits and both methods indicated an absence of metallic inclusions in the carbon solids. This is an essential step since metals such as iron and nickel have been found to be very active catalysts for the gasification of carbonaceous solids and this aspect would distort the oxidation profiles and create major problems with the characterization procedure [34].

2.3. Materials

The gases used in this work, C₂H₆, H₂, 1000 ppm and 5% H₂S/He, CO₂ and He, were all 99.999% purity and were purchased from MG and BOC Industries and used without further purification. Dimethyl sulfide (DMS) and dimethyl disulfide (DMDS) were

obtained from Aldrich. Research grade iron–nickel (1:4) powder was supplied by Johnson Matthey.

3. Results

3.1. Flow reactor studies

3.1.1. Effect of hydrogen sulfide on carbon deposition

In an attempt to establish a fundamental understanding of the relationship between the sulfur concentration in the reactant gas mixture and the potential for the formation of solid carbon in the ethane/steam system, experiments were performed under conditions where the reaction temperature was maintained constant and various concentrations of hydrogen sulfide were continuously added to the reactant feed passing over the powdered alloy samples. Analysis was conducted of the gaseous products and solid carbon yields obtained during the interaction of the Fe–Ni (1:4) alloy powder in an ethane/steam (4:1) environment as a function of the H_2S concentration at 815°C . These data which are presented in Fig. 1 show that the addition of as little as 25 ppm of H_2S result in a significant increase in the yield of solid carbon deposited on the iron–nickel alloy surface, while at the same time there is a corresponding decline in the generation of CO. The amount of CO is reduced still further upon raising the concentration of H_2S in the reactant. The solid carbon yield does

not appear to exhibit any pronounced change between 50 and 100 ppm H_2S , but eventually decreases when the sulfide concentration is raised above 100 ppm. The yields of the major gaseous products CH_4 and C_2H_4 increase as the level of H_2S is raised to 50 ppm and gradually decrease at higher additive levels.

In a further set of experiments with the iron–nickel/ethane–steam system, the concentration of H_2S was held constant at 150 ppm, whilst the temperature of the reaction was varied over the range 765 – 925°C . Inspection of the product distributions given in Fig. 2 indicates that the yield of solid carbon reaches a maximum at 865°C and then decreases at higher temperature. On the other hand, the concentration of the desired product, ethylene, exhibits a sharp drop as the temperature is raised from 765 to 815°C and continues to decrease upon reaching 925°C .

3.1.2. Effect of organicsulfides on carbon deposition

In this series of experiments the iron–nickel powder was initially reacted at 815°C in an ethane/steam (4:1) mixture containing various amounts of either DMS or DMDS. From a comparison of the data obtained with these respective sulfide additives, Figs. 3 and 4, it is evident that over the additive concentration range (25–150 ppm), in the presence of DMS the production of methane rises from 22 to 30%, but does not exhibit any dramatic changes with a DMDS additive. On the other hand, the yield of ethylene appears to reach

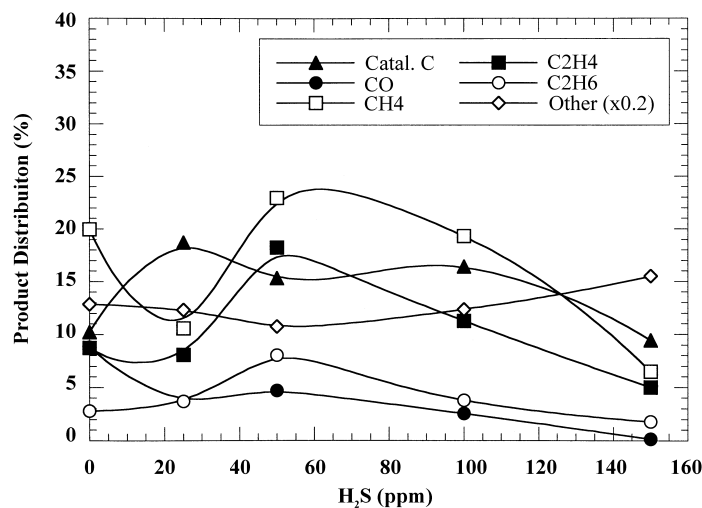


Fig. 1. Product distribution from the Fe–Ni (1:4) catalyzed decomposition of ethane/steam (4:1) containing various amounts of H_2S at 815°C .

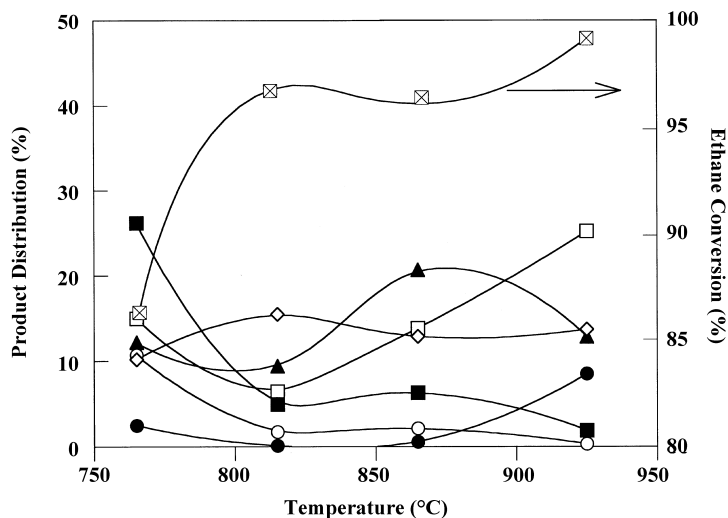


Fig. 2. Product distribution and percent conversion of ethane from the Fe-Ni (1:4) catalyzed decomposition of ethane/steam (4:1) containing 150 ppm H₂S as a function of temperature. (X) C₂H₆ conversion; (■) C₂H₄; (▲) solid C; (●) CO; (□) CH₄; (○) C₂H₆; (◇) Other (× 0.2).

an optimum level at 25–50 ppm DMS and 150 ppm DMDS. Startling differences in the solid carbon yields are found when the organic salts are used as the source of sulfur compared to the behavior observed with H₂S (Table 1). In the former cases no evidence for an enhancement in formation of carbon deposits is observed as a function of sulfide concentration and on

the contrary, it appears that at certain concentrations there is a decrease in the accumulation of such material. Furthermore, in systems where sulfur was derived from an organic precursor there is little variation of the mole fraction of ethane in the reactor effluent, suggesting that in these cases the conversion of the reactant was not affected by the sulfide concentration. A

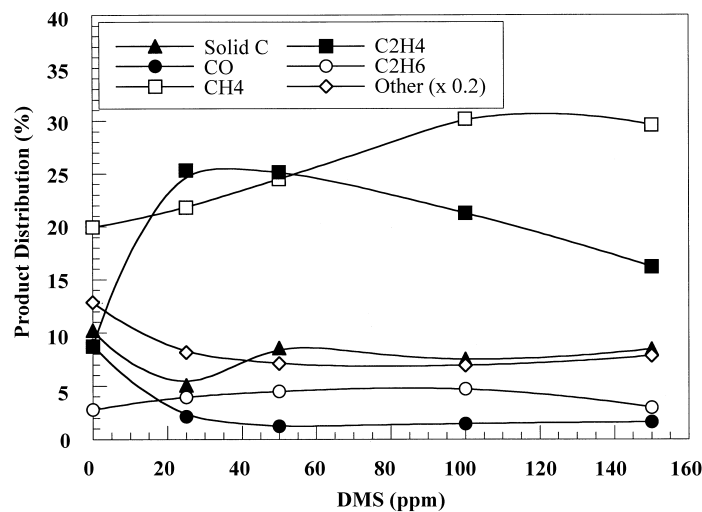


Fig. 3. Product distribution from the Fe-Ni (1:4) catalyzed decomposition of ethane/steam (4:1) containing various amounts of DMS at 815°C.

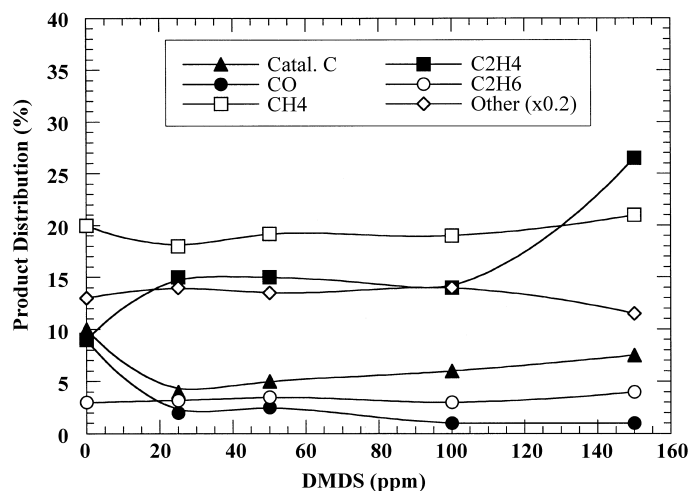


Fig. 4. Product distribution from the Fe–Ni (1:4) catalyzed decomposition of ethane/steam (4:1) containing various amounts of DMDS at 815°C.

comparison of the data presented in Tables 1 and 2 indicate that when the iron–nickel catalyzed decomposition of ethane is conducted at 815°C in the presence of the two organic sulfide additives an inverse relationship exists between the amount of carbon deposit and the yield of ethylene. In contrast, when the reaction is performed with the same concentrations of H₂S no distinct relationship is found between the yields of solid carbon and ethylene.

It is interesting to note that the effectiveness of both the inorganic and organic sulfides in suppressing catalytic carbon formation was indistinguishable as the concentration of each additive was progressively raised above 150 ppm. Experiments performed at additive levels in excess of 500 ppm showed that the yield of solid carbon was the same with all three sulfide compounds.

Table 1

Comparison of percent solid carbon yield from the iron–nickel catalyzed decomposition of ethane at 815°C as a function of the concentration of various sulfide additives

Concentration of additive (ppm)	H ₂ S	DMS	DMDS
0	10.1	10.1	10.1
25	18.8	5.1	3.8
50	15.6	8.1	4.9
100	16.5	7.5	5.9
150	8.7	8.0	8.5

Table 2

Comparison of the ethylene yields from the iron–nickel catalyzed decomposition of ethane at 815°C as a function of the concentration of various sulfide additives

Concentration of additive (ppm)	H ₂ S	DMS	DMDS
0	8.8	8.8	8.8
25	7.9	25.5	15.0
50	17.9	25.0	15.0
100	10.8	20.2	12.6
150	5.0	16.7	25.8

Finally, the effect of reaction temperature on the performance of the organically derived sulfur on inhibiting the growth of solid carbon was investigated. The results of experiments performed in the presence of 150 ppm of each additive as function of temperature over the range 765–925°C as given in Fig. 5 (DMS) and Fig. 6 (DMDS). When the interaction of the iron–nickel powder with ethane/steam was carried out in mixtures containing 150 ppm DMDS, the yield of solid carbon exhibited a decrease as the temperature was progressively increased from 765 to 925°C. This trend was not so apparent when an analog set of experiments were carried out in the presence of 150 ppm DMS. From a comparison of the data contained in these two plots, it was interesting to find that in the presence of DMS, the ethylene selectivity decreased as a function of increasing temperature, Fig. 5, whereas at 815°C an optimum yield of the olefin is

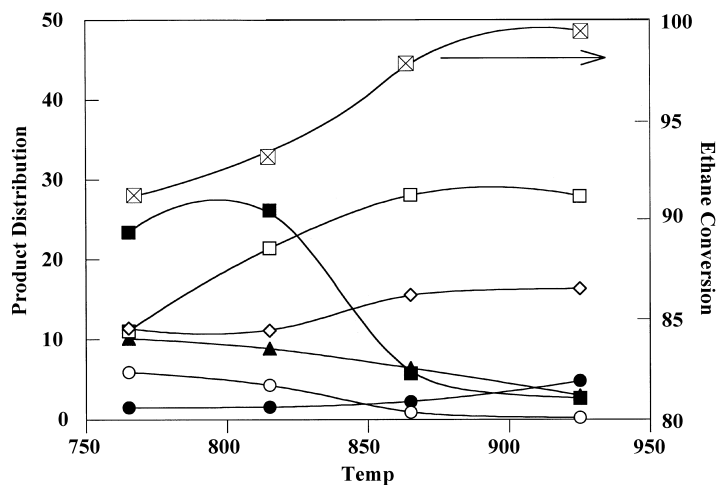


Fig. 5. Product distribution and percent conversion of ethane from the Fe-Ni (1:4) catalyzed decomposition of ethane/steam (4:1) containing 150 ppm DMS as a function of temperature. (⊠) C₂H₆ conversion; (■) C₂H₄; (▲) solid C; (●) CO; (□) CH₄; (○) C₂H₆; (◇) Other (× 0.2).

achieved upon addition of 150 ppm of DMDS to the reactant mixture (Fig. 6).

3.2. Characterization studies of the solid carbon deposit

3.2.1. Temperature programmed oxidation studies

The oxidation profiles of the demineralized carbon deposits generated from the interaction of

ethane/steam (4:1) mixture containing 25–150 ppm of the, respective, sulfides with Fe-Ni powders at 815°C for 2 h are shown in Figs. 7–9. For comparison purposes, included on each plot is the profile obtained for the solid carbon produced in the absence of sulfide additives under otherwise identical reaction conditions. It is apparent that in the case of H₂S, the oxidation profiles are found to be highly dependent upon the partial pressure of sulfur in the

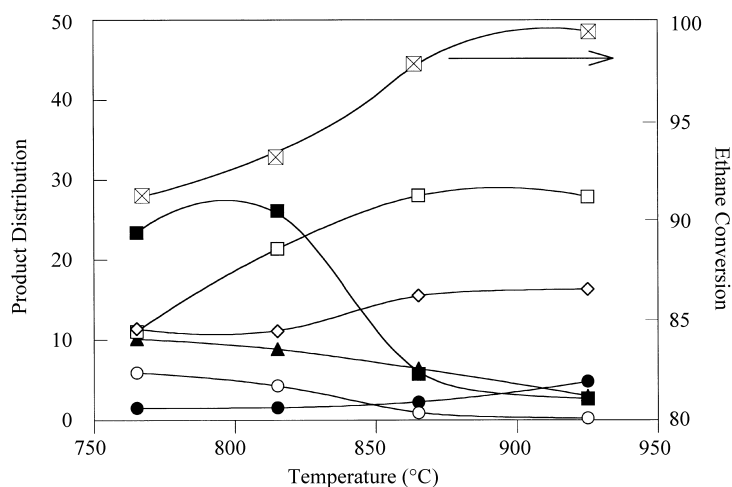


Fig. 6. Product distribution and percent conversion of ethane from the Fe-Ni (1:4) catalyzed decomposition of ethane/steam (4:1) containing 150 ppm DMDS as a function of temperature. (⊠) C₂H₆ conversion; (■) C₂H₄; (▲) solid C; (●) CO; (□) CH₄; (○) C₂H₆; (◇) Other (× 0.2).

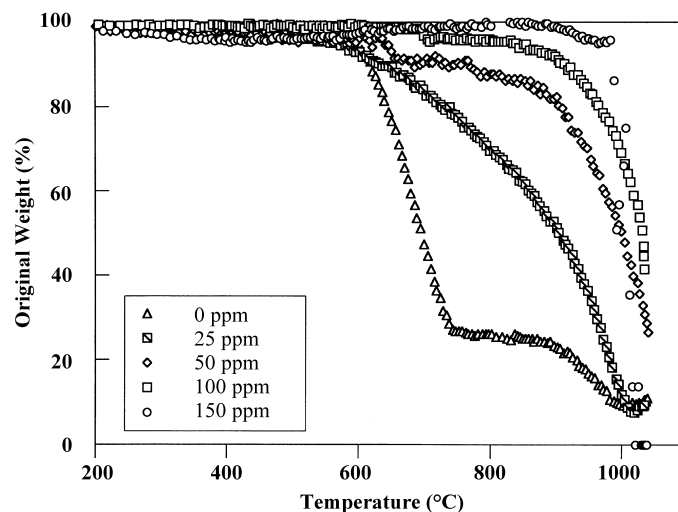


Fig. 7. Comparison of the gasification characteristics in CO_2/Ar (1:1) of catalytic carbon produced from the interaction of Fe–Ni (1:4) alloy at 815°C with $\text{C}_2\text{H}_6/\text{H}_2\text{O}$ (4:1) containing various concentrations of H_2S .

gaseous reactant stream. In general, however, as the level of sulfur in the reactant gas is raised, the carbon deposits produced from the iron–nickel catalyzed decomposition of ethane at 815°C become progressively more graphitic in nature. This feature is particularly evident with the solid carbon generated in the presence of all concentrations of the organic

sulfides, which are found to be significantly more graphitic in nature than those produced when equivalent concentrations of H_2S were present in the reactant gas.

In a final set of experiments, the influence of reaction temperature on the character of the carbon deposits produced from ethane/steam mixtures con-

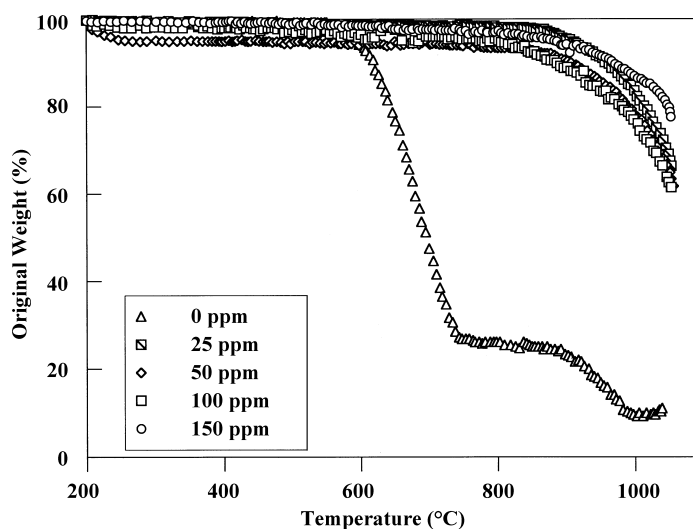


Fig. 8. Comparison of the gasification characteristics in CO_2/Ar (1:1) of catalytic carbon produced from the interaction of Fe–Ni (1:4) alloy at 815°C with $\text{C}_2\text{H}_6/\text{H}_2\text{O}$ (4:1) containing various concentrations of DMS.

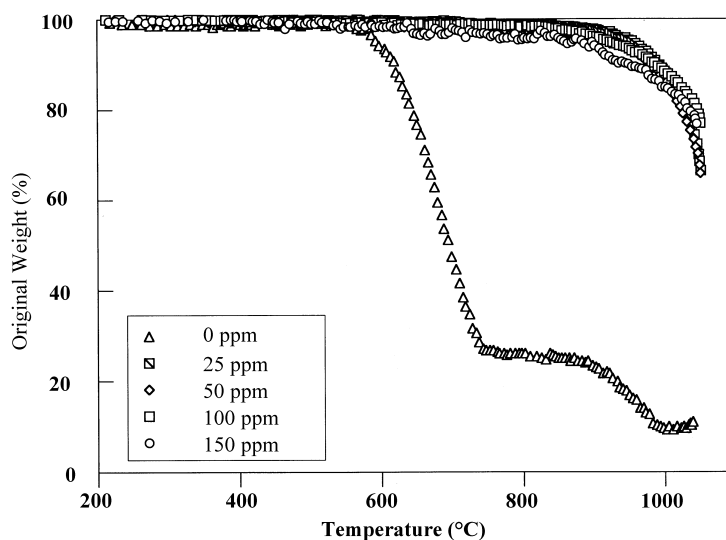


Fig. 9. Comparison of the gasification characteristics in CO_2/Ar (1:1) of catalytic carbon produced from the interaction of Fe–Ni (1:4) alloy at 815°C with $\text{C}_2\text{H}_6/\text{H}_2\text{O}$ (4:1) containing various concentrations of DMDS.

taining 150 ppm DMDS was investigated. For this purpose the concentration of the organic sulfide additive was held constant at 150 ppm, while the temperature was varied over the range 765 – 925°C . From the profiles shown in Fig. 10 it is clear that the carbonaceous material acquired a more graphitic character as

the reaction temperature was increased, reaching the highest level at 925°C .

3.2.2. Transmission electron microscopy studies

Examination by transmission electron microscopy of the structures of the carbon deposits that were

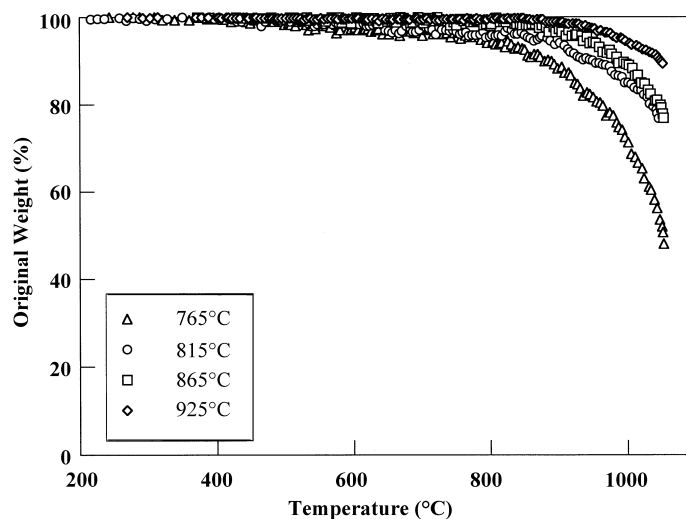


Fig. 10. Comparison of the gasification characteristics in CO_2/Ar (1:1) of catalytic carbon produced from the interaction of Fe–Ni (1:4) alloy with $\text{C}_2\text{H}_6/\text{H}_2\text{O}$ (4:1) containing 150 ppm of DMDS at various temperatures.

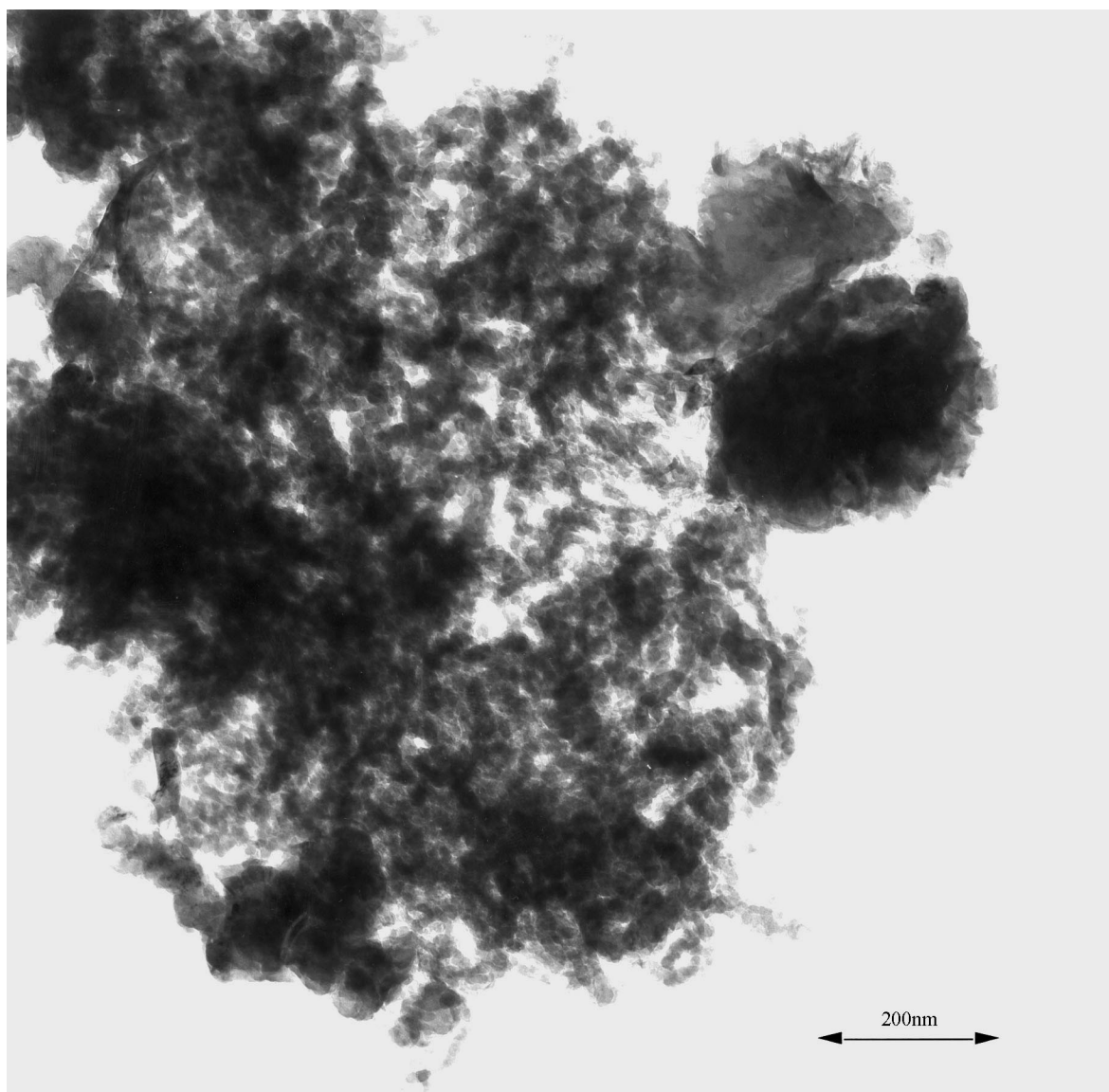


Fig. 11. Transmission electron micrograph of carbon filaments produced from the interaction of $\text{C}_2\text{H}_6/\text{H}_2\text{O}$ (4:1) over Fe–Ni (1:4) alloy particles at 765°C in the presence of 150 ppm DMDS.

produced on the iron–nickel powdered catalysts from the various reaction systems revealed the existence of two types of material: carbon filaments and graphite “shell-like” structures. Filamentous carbon deposits were found in the greatest abundance at 765 and 865°C and the typical appearance of these structures is presented in the electron micrographs (Figs. 11–13).

A more detailed appreciation of an individual carbon filament and the associated iron–nickel particle can be seen in Fig. 14. This type of structure was produced from an ethane–steam reactant mixture containing 150 ppm of H_2S and has been generated by the “whisker-like” mode where the catalyst is located at the growing end of the filament. When

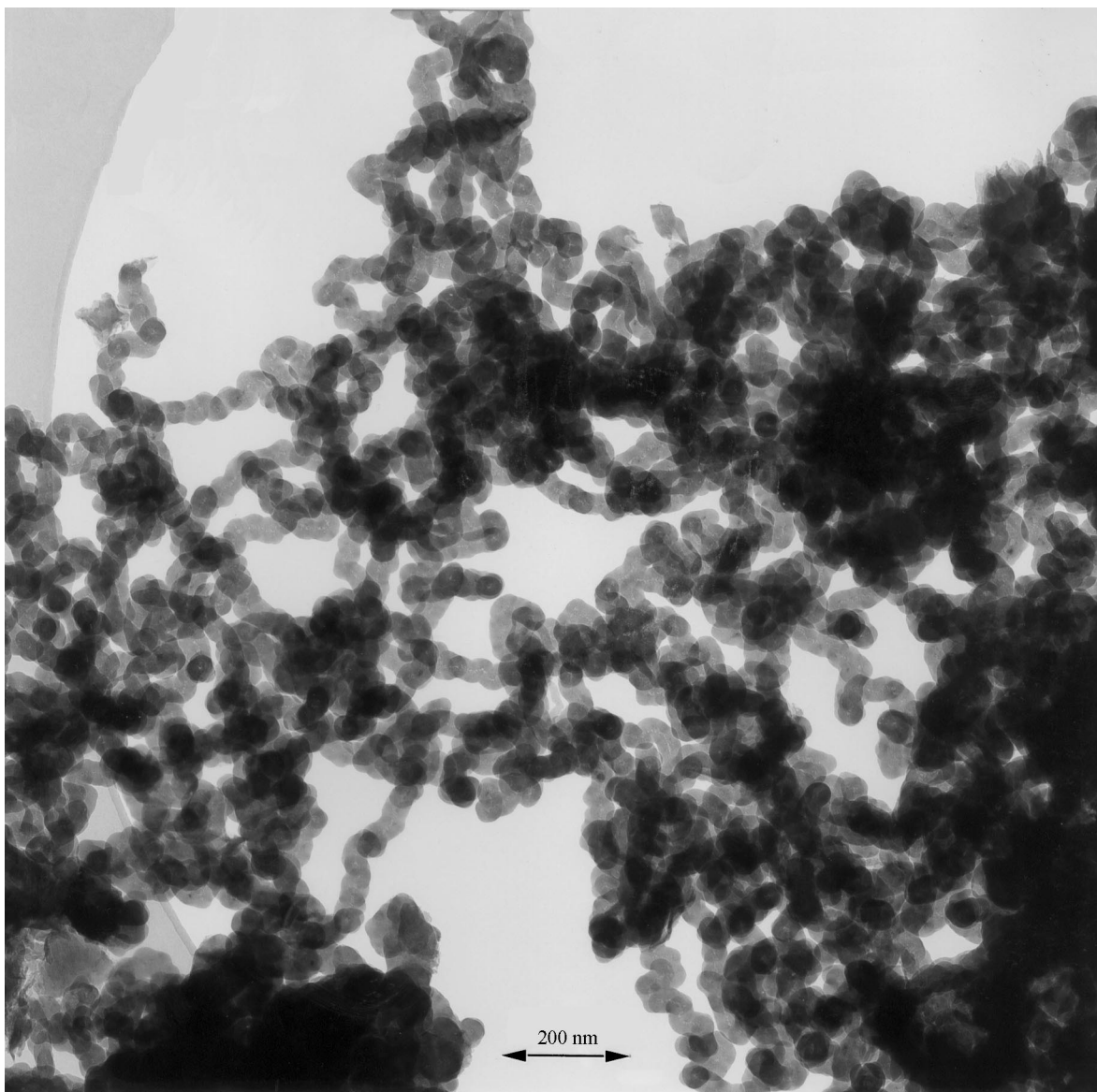


Fig. 12. Transmission electron micrograph of carbon filaments produced from the interaction of $\text{C}_2\text{H}_6/\text{H}_2\text{O}$ (4:1) over Fe–Ni (1:4) alloy particles at 815°C in the presence of 150 ppm DMDS.

H_2S was replaced by either of the organic sulfides the amount of carbon filaments was significantly reduced, nevertheless the structural characteristics were identical to those described above. High resolution examination shows that these filaments possess a well-defined ordered structure and from the appearance of the lattice fringe images it is possible to

ascertain that the graphite platelets are aligned in a direction that is almost parallel to the fiber axis (Fig. 15). In sharp contrast, the carbon filaments formed from an ethane-steam mixture that did not contain any sulfur additives tended to acquire a more disordered “bead-like” structure, an example of which is presented in the electron micrograph (Fig. 16).

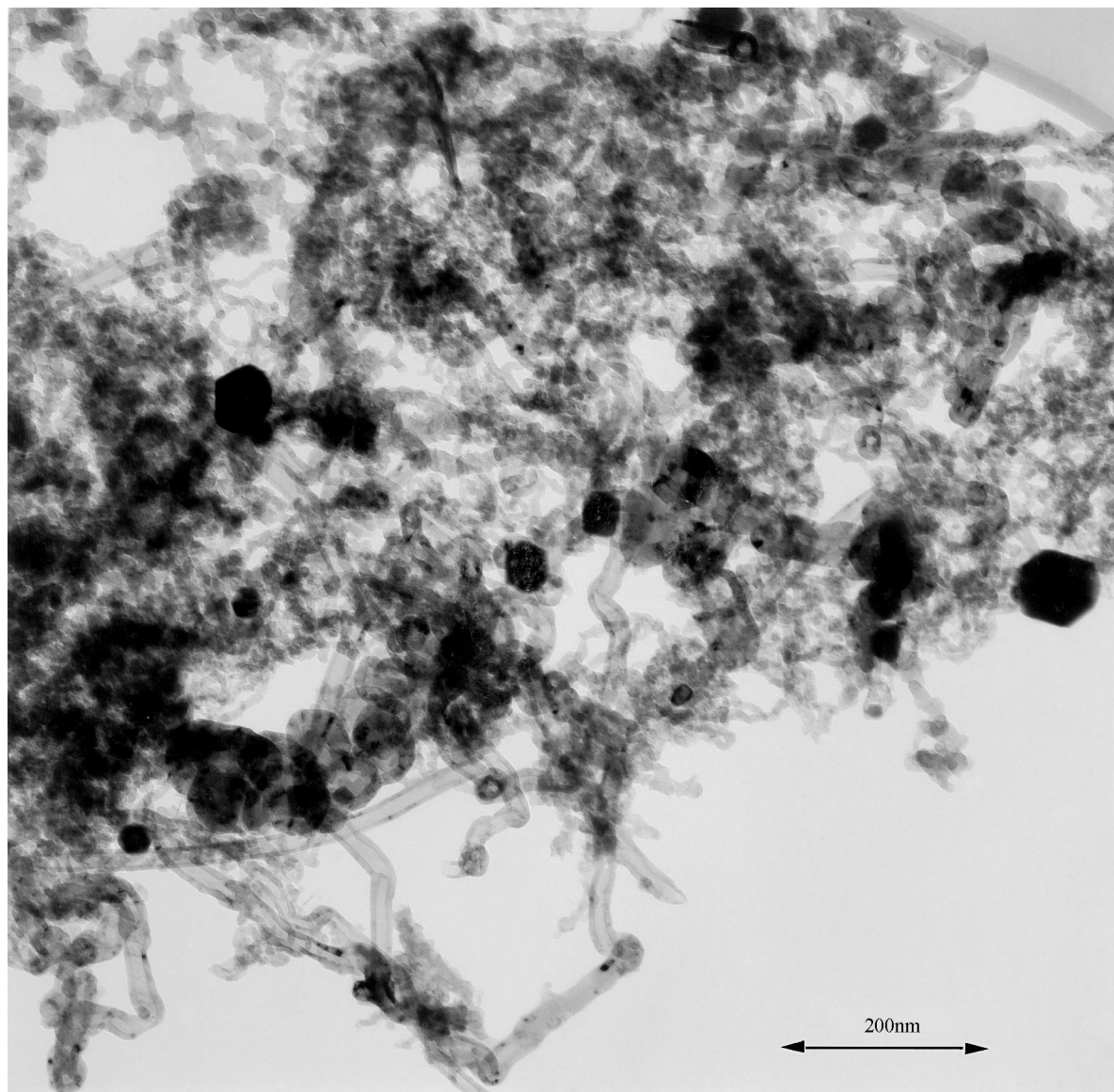


Fig. 13. Transmission electron micrograph of carbon filaments produced from the interaction of $\text{C}_2\text{H}_6/\text{H}_2\text{O}$ (4:1) over Fe–Ni (1:4) alloy particles at 865°C in the presence of 150 ppm DMDS.

The other type of deposit, a shell-like material in which iron–nickel particles appeared to be coated and encapsulated by highly graphitic carbon, is shown in Fig. 17. Electron diffraction studies confirmed that this material possessed a high degree of crystalline perfection. This form of carbon tended to predominate at 925°C and was most prevalent in the deposits

associated with the presence of organic sulfides in the reactant stream. It was interesting to find, however, that the amount of the shell-like deposit produced on a given alloy particle was significantly lower than that achieved when a similar sized catalyst particle was responsible for generating filamentous carbon structures.



Fig. 14. Transmission electron micrograph showing the appearance of a carbon filament and the associated catalyst particle produced after reaction at 865°C with an $\text{C}_2\text{H}_6/\text{H}_2\text{O}$ (4:1) mixture containing 150 ppm H_2S .

4. Discussion

It is apparent from this investigation that significant differences were observed when the Fe–Ni (1:4) samples were heated in an ethane–steam reactant mixture containing similar concentrations of either H_2S , DMS or DMDS. From examination of the data given in Tables 1 and 2 it is apparent that the yields of catalytic carbon deposits and ethylene are extremely sensitive to the concentration as well as the chemical nature of sulfide additive. In the 25–150 ppm range, the major difference between H_2S , DMDS and DMS is that whereas the former additive promoted carbon deposition, both organic sulfides suppressed this process on the alloy. Furthermore, it can be seen that the performance of DMDS in this regard was superior to that displayed by DMS at concentrations up to 150 ppm. Analysis of the total products derived from experiments where the organic sulfides were introduced into the reactant mixture reveals that as the accumulation of solid carbon decreases there is a corresponding enhancement in the yield of ethylene. This finding is consistent with the notion that catalytic carbon is formed via a secondary reaction, i.e. the catalyzed decomposition of ethylene.

The diverse behavior displayed by the inorganic and organic sulfur compounds is fascinating and leads one to conclude that contrary to the accepted view in these reactions the organic sulfides do not readily undergo gas phase decomposition and merely function as an expensive source of H_2S , but instead retain some of their organic characteristics when they adsorb on the alloy surfaces. Moreover, the subtle differences observed with DMS and DMDS suggest that the nature of the organic functionality plays a critical role in the performance of the sulfur moiety with regard to inhibition of carbon deposition and selectivity towards ethylene formation. Further, surface studies are being conducted on these systems in an attempt to elucidate the difference in adsorption characteristics between H_2S and the organic sulfides on the alloy.

Since sulfur chemisorption on metal surfaces either prevents or modifies the adsorption characteristics of other reactant molecules, in many respects it resembles the behavior of certain metallic additives, such as copper, in bimetallic catalysts [24]. Sulfur adsorption on a metal surface causes two types of poisoning: (a) blockage of catalytic sites (geometric effect) and (b) changes in the catalytic performance of the host due to the influence of neighboring sulfur atoms (electronic

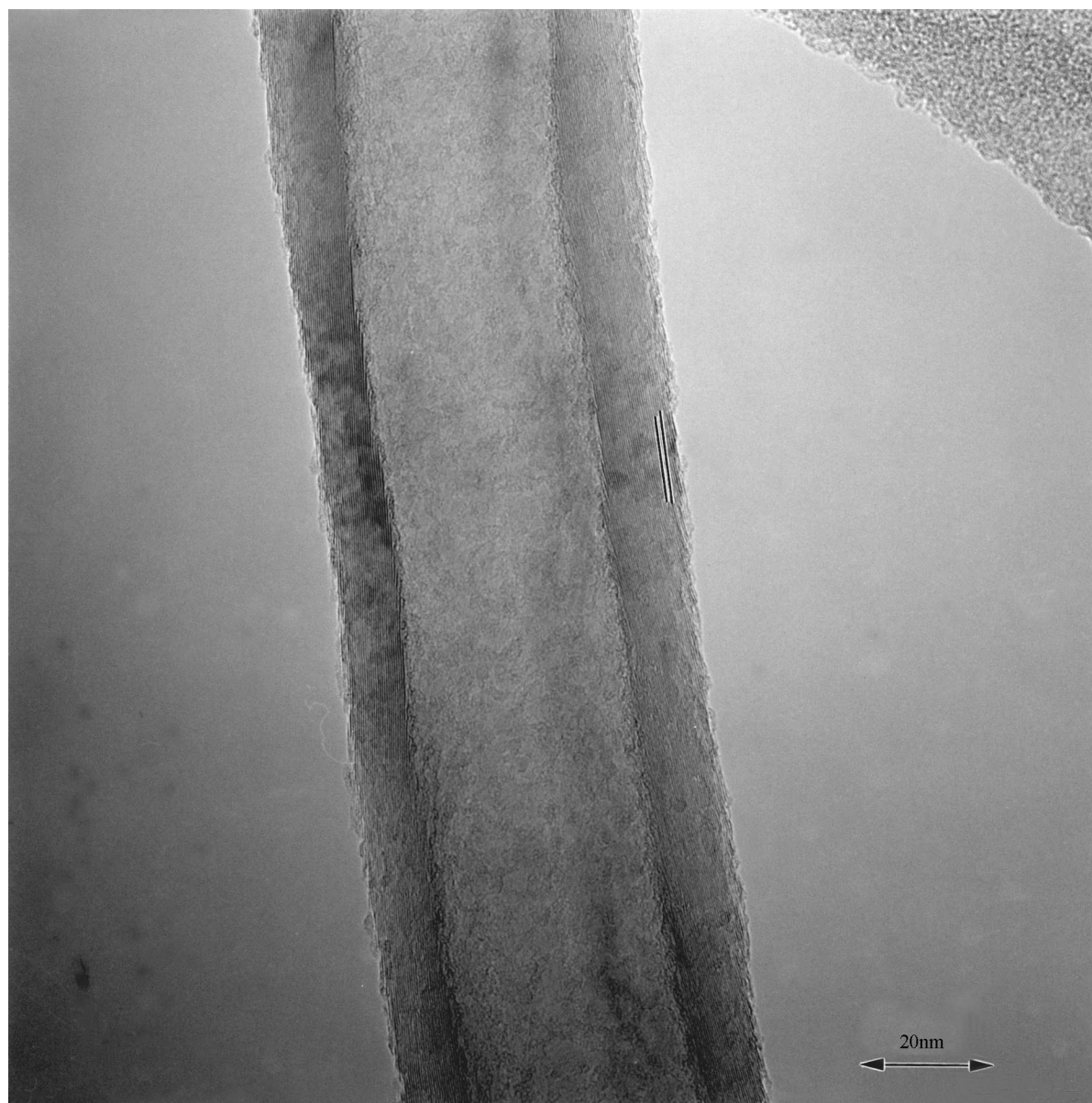


Fig. 15. High resolution transmission electron micrograph showing the details of the lattice fringe image of the graphite platelets (the direction is indicated by parallel lines) constituting the carbon filament presented in Fig. 14.

effect). The geometric effect plays an important role over the entire sulfur coverage range and dominates in the high coverage regions [24,35,36]. On the other hand, the electronic effect is considered to be operative only at low sulfur coverages [37,38]. Somorjai [39]

proposed that facile (small ensemble) reactions such as hydrogenation and dehydrogenation should be less affected by sulfur addition than demanding (large ensemble) reactions like hydrogenolysis. Consequently, a sulfur treatment of metal catalysts may provide a

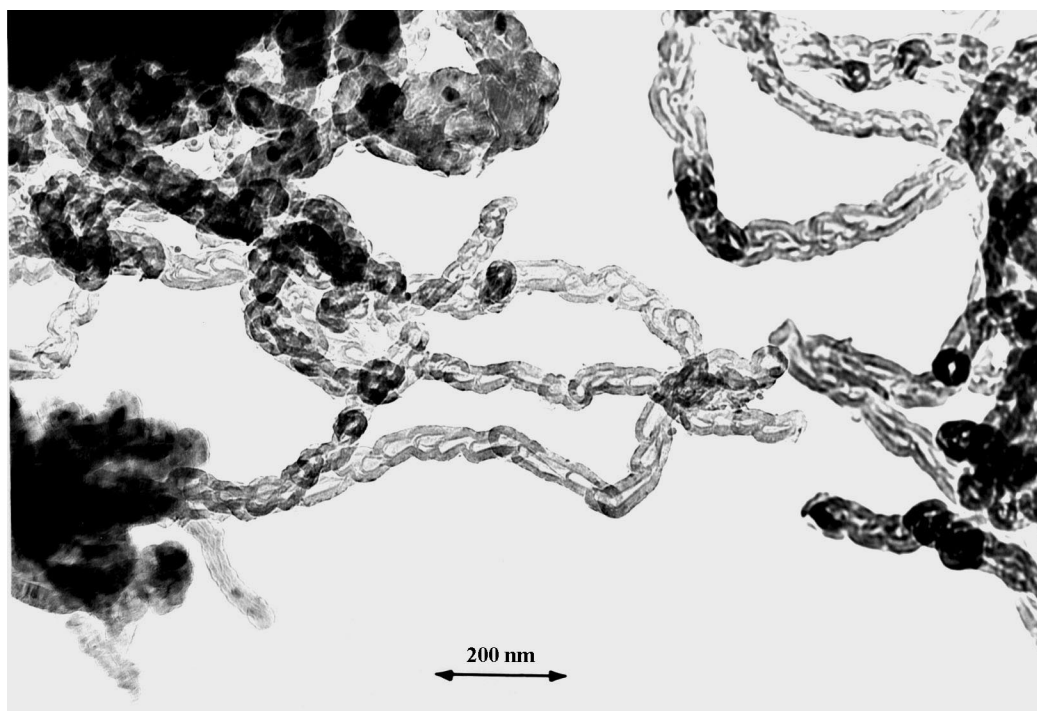


Fig. 16. Transmission electron micrograph showing the appearance of carbon filaments produced after reaction at 925°C from interaction of Fe–Ni (1:4) alloy particles with an $\text{C}_2\text{H}_6/\text{H}_2\text{O}$ (4:1) mixture.

sensitive tool for improving selectivity by modifying the concentration of ensembles [40].

Another aspect that can be encountered with sulfur addition is the possibility of reconstruction of the metal surfaces. The phenomenon of surface reconstruction or faceting is important in catalysis, especially in regard to structure-sensitive reactions. Sulfur induced reconstruction has been rationalized in two ways [41]: (a) a change in the cooperative stable condition as a result of hydrogen desorption and (b) a modification in the metal–sulfur bonding characteristics to accommodate more sulfur atoms. Presumably, a strong metal–sulfur interaction weakens the bonding between the surface and the next lower metal layers, allowing for rearrangements of the surface metal atoms to take place. In this regard one might expect to find a difference in the strength of such bonding when sulfur is derived from an organic rather than an inorganic compound. Furthermore, it is possible that the structure of the organic sulfides plays a critical role in the adsorption step and the characteristics of this

process may be quite different to those encountered with H_2S . Clearly, these aspects warrant further fundamental study and a detailed surface science investigation of the interactions may reveal the key factors surrounding the differences in adsorption and subsequent decomposition behavior of H_2S and the organic sulfides.

The results of electron microscopy examinations demonstrated that the addition of sulfur species to the reactant feed exerted a profound influence on the characteristics of the catalytically generated carbon filaments. When one combines these studies with the TPO data presented in Figs. 7–9, it becomes evident that the presence of sulfur, particularly that derived from the organic precursors, induces a significant influence on the crystalline perfection of the carbon filaments. Since this property is directly related to the events occurring at the metal–carbon interface [13–16] it is tempting to speculate that sulfur has an impact on the interstitial spacing of the metal atoms in this region, thereby creating an improvement in the registry

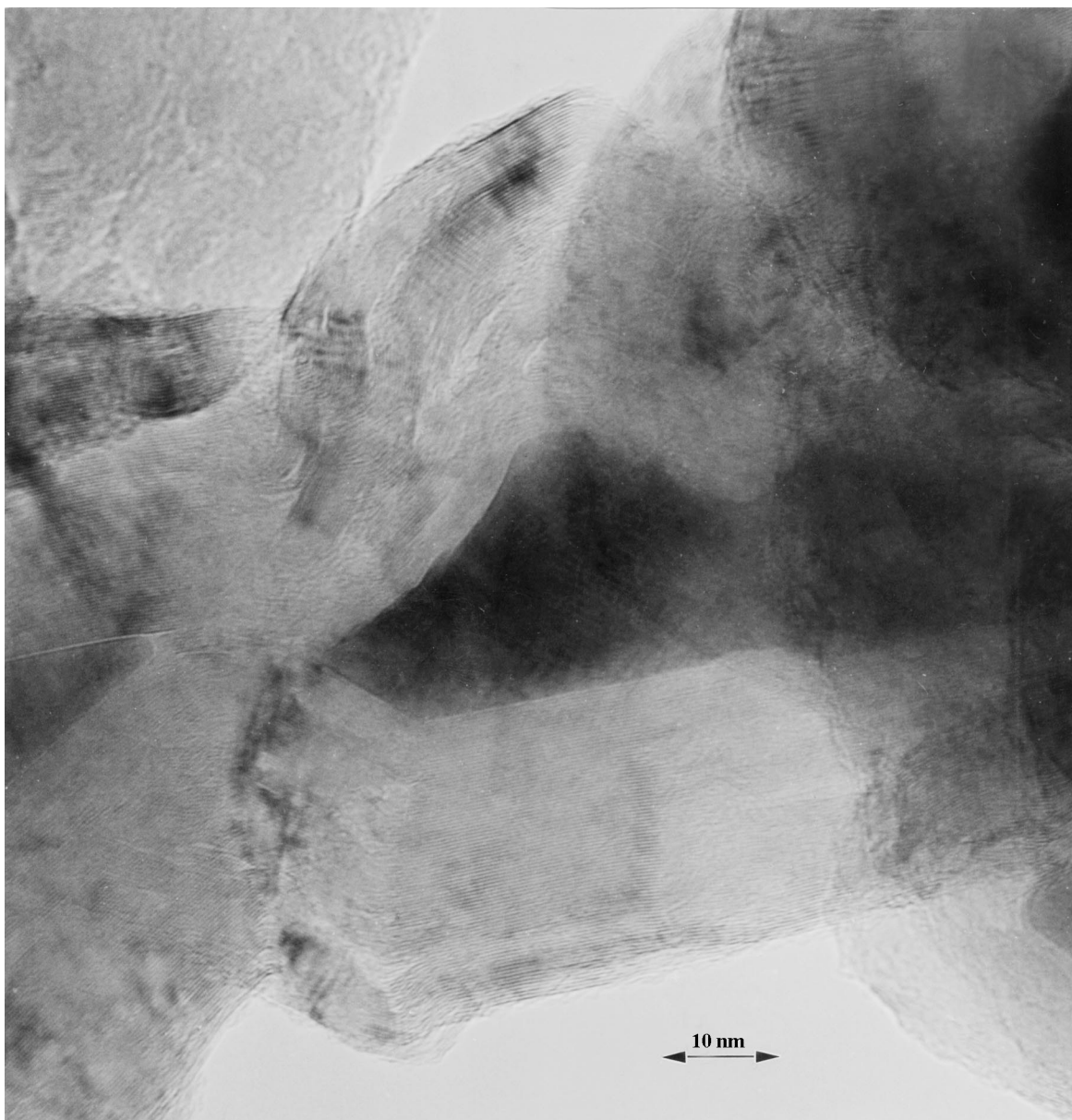


Fig. 17. Transmission electron micrograph of the graphitic shell-like deposit formed on Fe–Ni (1:4) particles during the interaction with an $\text{C}_2\text{H}_6/\text{H}_2\text{O}$ (4:1) mixture containing 150 ppm DMS at 925°C .

with the interatomic distance of the carbon–carbon bond in graphite. The observation that many of the carbon filaments adopt identical crystalline structures to the “recently discovered” multi-walled carbon nanotubes confirms the opinion held by many

researchers that these types of deposits have been known for many years and are universally regarded as a nuisance in the efficient operation of many industrial processes that involve hydrocarbon conversion reactions.

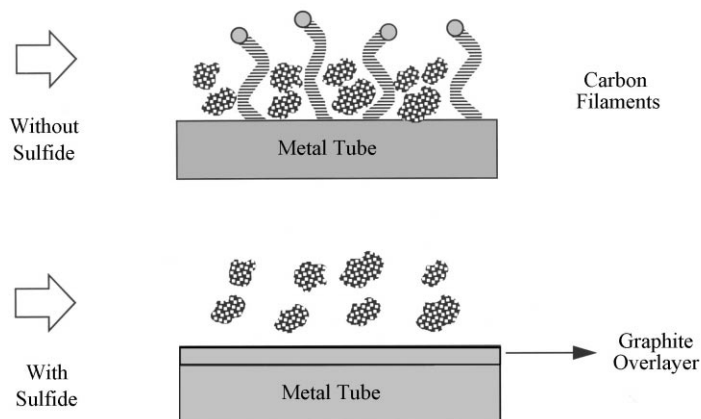


Fig. 18. Schematic representation of the transformation in the nature and structure of the carbonaceous deposit as the temperature is raised to 925°C.

In all cases it was found that as the temperature was progressively raised from 865 to 925°C there was a distinct change in the form of the deposit. This transformation in the character of the solid carbon deposit from filamentous structures to a shell-like geometry that is observed when the alloy is treated at temperatures in excess of 865°C in a reactant mixture containing the organic sulfides may have some important technological ramifications. Consider the situation depicted in the schematic diagram in Fig. 18. In the absence of a sulfide additive, carbon filaments are formed at a rapid rate during the initial stages of the cracking reaction. Over a period of time these structures provide a high surface area collection site for pyrolytic carbon, derived from uncatalyzed gas phase reactions. Essentially, the combination of these two processes generates the required conditions for the formation of a carbon–carbon composite that possesses a high mechanical strength and as consequence, is difficult to remove from the reactor walls. In contrast, it would appear that in the presence of a suitable concentration of a sulfide additive, the growth of filamentous carbon is restricted in favor of the formation of a smooth graphite sheet deposit, which does not provide the type of surface that is conducive for the accumulation of the pyrolytic carbon component. Under these conditions there is a net decrease in the overall amount of carbon deposited and the highly graphitic nature of the shell-like material would be less likely to exert a deleterious effect with respect to the heat transfer

properties within the metal reactor tube. In addition, the preferential formation of this latter type of deposit will tend reduce the likelihood of encountering the problems associated with the extensive collection of pyrolytic carbon derived from non-catalyzed sources that invariably result in blockage of the reactor.

Acknowledgements

This work was supported by a grant from Elf Atochem North America Inc. The authors would like to thank Prof. Nelly Rodriguez (Chemistry Department, Northeastern University) and Dr. M.J. Lindstrom and his colleagues at Elf Atochem North America Inc., King of Prussia, PA for their helpful discussions.

References

- [1] L.J.E. Hofer, in: P.H. Emmett. (Ed.), *Catalysis*, Vol. 4, Reinhold Publishing, New York, 1956, p. 373.
- [2] H.B. Palmer, C.F. Cullis, in: P.L. Walker Jr. (Ed.), *Chemistry and Physics of Carbon*, Vol. 1, Marcel Dekker, New York, 1965, p. 265.
- [3] J.R. Rostrup-Nielsen, *Steam Reforming Catalysts*, Tekorisk Forlay A/S, Danish Technical Press, 1975.
- [4] D.L. Trimm, *Catal. Rev.-Sci. Eng.* 16 (1977) 155.
- [5] R.T.K. Baker, P.S. Harris, in: P.L. Walker Jr., P.A. Thrower (Eds.), *Chemistry and Physics of Carbon*, Vol. 14, Marcel Dekker, New York, 1978, p. 83.

- [6] C.H. Bartholomew, *Catal. Rev.-Sci. Eng.* 24 (1982) 67.
- [7] R.T.K. Baker, in: J.L. Figueiredo et al. (Eds.), *Carbon Fibers Filaments and Composites*, NATO ASI Series, Kluwer Academic Publishers, Dordrecht, 177, 1990, p. 405.
- [8] N.M. Rodriguez, *J. Mater. Sci.* 8 (1993) 3233.
- [9] J. Lahaye, P. Bodie, J. Ducret, *Carbon* 15 (1977) 87.
- [10] J.B. Butt, *Adv. Chem. Ser.* 109 (1972) 259.
- [11] R.T.K. Baker, M.A. Barber, F.S. Feates, P.S. Harris, R.J. Waite, *J. Catal.* 26 (1972) 51.
- [12] I. Alstrup, *J. Catal.* 109 (1988) 241.
- [13] M. Audier, A. Oberlin, M. Oberlin, M. Coulon, L. Bonnetain, *Carbon* 19 (1981) 217.
- [14] R.T. Yang, J.P. Chen, *J. Catal.* 115 (1989) 52.
- [15] M.S. Kim, N.M. Rodriguez, R.T.K. Baker, *J. Catal.* 134 (1992) 253.
- [16] N.M. Rodriguez, A. Chambers, R.T.K. Baker, *Langmuir* 11 (1995) 3862.
- [17] P.E. Nolan, D.C. Lynch, A.H. Cutler, *Carbon* 32 (1994) 477.
- [18] N.M. Rodriguez, M.S. Kim, F. Fortin, I. Mochida, R.T.K. Baker, *Appl. Catal. A* 148 (1997) 265.
- [19] M.S. Kim, N.M. Rodriguez, R.T.K. Baker, *J. Catal.* 143 (1993) 449.
- [20] W.T. Owens, N.M. Rodriguez, R.T.K. Baker, *Catal. Today* 21 (1994) 3.
- [21] W.T. Owens, M.S. Kim, N.M. Rodriguez, R.T.K. Baker, in: B. Delmon, G.F. Froment (Eds.), *Catalyst Deactivation 1994*, Elsevier, Amsterdam, 1994, p. 191.
- [22] D.L. Trimm, A. Holmen, O.J. Lindvag, *Chem. Tech. Biotechnol.* 31 (1981) 311.
- [23] H.S. Swift, H. Beuther, R.J. Rannard, *Ind. Eng. Chem. Prod. Res. Div.* 15 (1976) 131.
- [24] J.R. Rostrup-Nielsen, *J. Catal.* 85 (1984) 31.
- [25] D.L. Trimm, C.J. Turner, *J. Chem. Tech. Biotechnol.* 31 (1981) 285.
- [26] D.C. Gardiner, C.H. Bartholomew, *Ind. Eng. Chem. Prod. Res. Div.* 20 (1981) 80.
- [27] G.F. Froment, *Rev. Chem. Eng.* 16 (1990) 295.
- [28] M.S.G. Reyniers, G.F. Froment, *Ind. Eng. Chem. Res.* 34 (1995) 773.
- [29] M. Kawaguchi, K. Nozaki, S. Motojima, H. Iwanaga, *J. Cryst. Growth* 118 (1992) 309.
- [30] S. Motojima, I. Hasegawa, S. Kagiya, M. Momiyama, M. Kawaguchi, H. Iwanaga, *Appl. Phys. Lett.* 62 (1993) 2322.
- [31] T. Kato, K. Haruta, K. Kusakabe, S. Morooka, *Carbon* 30 (1992) 989.
- [32] H. Katsuki, K. Matsunaga, M. Egashira, S. Kawasumi, *Carbon* 19 (1981) 148.
- [33] M. Egashira, H. Katsuki, Y. Ogawa, S. Kawasumi, *Carbon* 21 (1983) 89.
- [34] R.T.K. Baker, J.J. Chludzinski, R.D. Sherwood, *Carbon* 23 (1985) 245.
- [35] M. George, R.B. Moyes, D. Ramanaro, P.B. Wells, *J. Catal.* 52 (1978) 486.
- [36] W.D. Fitzharris, J.R. Katzer, W.H. Manogue, *J. Catal.* 76 (1982) 369.
- [37] M. Kiskinova, D.W. Goodman, *Surf. Sci. L* 105 (1981) 265.
- [38] M. Kiskinova, D.W. Goodman, *Surf. Sci.* 108 (1981) 64.
- [39] G.A. Somorjai, *J. Catal.* 27 (1972) 453.
- [40] J.R. Rostrup-Nielsen, in: C.H. Bartholomew, J.B. Butt (Eds.), *Catalyst Deactivation*, Elsevier, Amsterdam, 1991, p. 85.
- [41] C.H. Bartholomew, P.K. Agrawal, J.R. Katzer, *Adv. Catal.* 31 (1982) 135.